SUPPORTING INFORMATION FOR:

Stress-aided thermal activation of crack propagation in multidentate hydrogen bonding adhesives

Zachary D. Lamberty[1,2], Ngon T. Tran[3], Daniel B. Knorr, Jr [3], and Joelle Frechette[1,4,*]

1. Chemical and Biomolecular Engineering Department, University of California, Berkeley, Berkeley, California 94760, USA.
2. US Naval Research Laboratory Chemistry Division, Code 6176, 4555 Overlook Ave, SW, Washington, DC 20375, USA.
3. *DEVCOM* U.S. Army Research Laboratory, Aberdeen Proving Ground, Maryland 21005, USA.
4. Energy Storage and Distributed Resources Division, Lawrence Berkeley National Laboratory, Berkeley, CA 94720, USA.

***Corresponding author:** Joelle Frechette jfrechette@berkeley.edu

1. ATR-FTIR Spectra

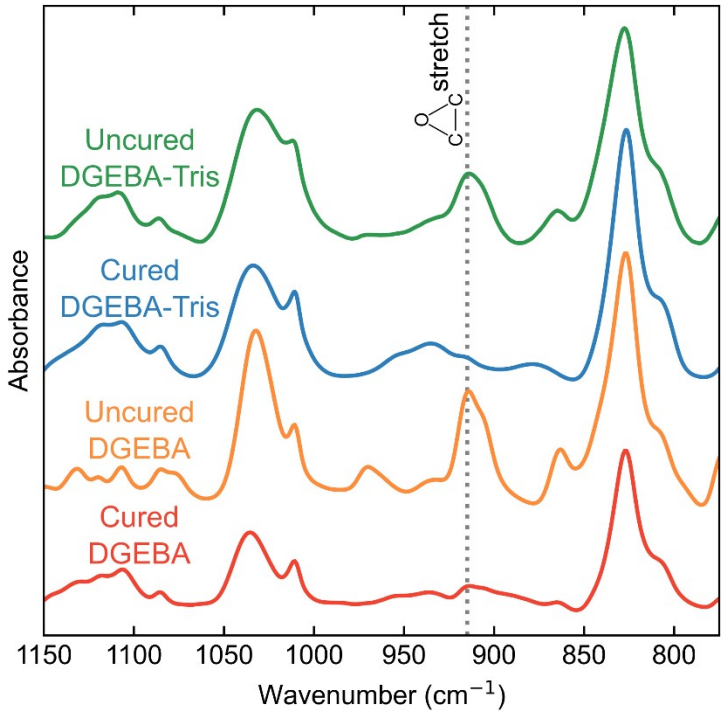

Figure S1. ATR-FTIR spectra in the epoxide stretch region of DGEBA and DGEBA-Tris over varying cure times. (a) IR spectra of DGEBA-Tris uncured (green, top) and cured at 200 °C for 4 h (blue, 2nd from top), as well as uncured DGEBA (orange, 2nd from bottom) and DGEBA cured at 220 °C for 16 h (red, bottom). Dashed vertical lines indicate the characteristic asymmetric vibration peak of an epoxide ring at 915 cm^{-1}. Spectra are shifted vertically for clarity.

2. Experimental set up for temperature-controlled self-arresting crack measurements

Performing self-arresting crack propagation measurements at temperatures other than room temperature requires the development of an experimental set up with temperature control, as previous setups performed tests without temperature control on an inverted microscope.[11,32] To heat samples reliably, an apparatus was built around a hot plate sample stage (**Fi.g S2a**), allowing for precise control of the sample temperature. Samples were held down using steel blocks to prevent sliding, while a pair of steel rods attached to a micrometer were utilized to move the glass spacer (**Fig S2b**). The camera and associated optics were affixed to a microstepping motor, allowing for translation of the camera frame without affecting the sample. Tests revealed that the temperature at the hot plate surface and at the top of a mica sample reliably differed by no more than 1 °C over the range of interest and remained stable for hours once equilibrated.

Cooling of the sample was achieved by replacing the hot-plate sample stage with a water-tight steel chamber (**Fig S2c**), which itself is connected to a recirculating ice water bath, providing a constant flow of 0 °C water in and out of the chamber. The samples were then mounted on top of the chamber, allowing for good thermal contact with the reservoir without directly exposing the samples to water. After equilibration, the sample platform surface reliably reached 8 – 9 °C. To prevent condensation, the entire apparatus was then enclosed in a sealed box under a constant purging of N_2. Dishes of desiccant were also placed near the samples and the manipulation of the sample was kept at a minimum to minimize intrusion of ambient humidity. Experiments were conducted at less than 30% relative humidity (measured at 20 °C), at which point no condensation was observed on (or around) the samples.

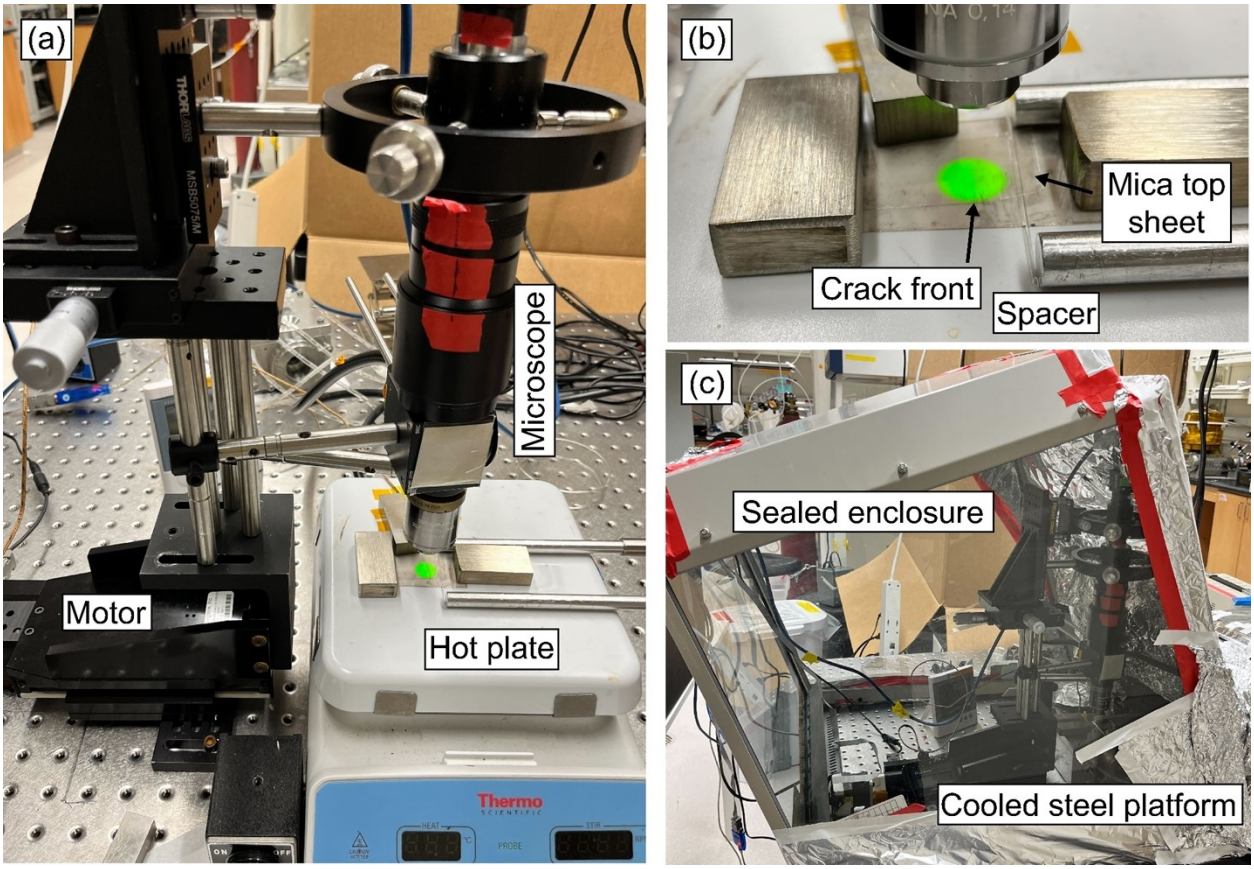

Figure S2. Experimental setup. (a) photo of the experimental apparatus for heated tests, showing the translating motor attached to the microscope, camera, and light source, as well as the hot plate and sample. (b) close up photo of the sample, showing the spacer bending the top mica sheet upwards, creating a crack. (c) photo of the setup for cooled experiments, where the sample is placed on a cooled steel platform

connected to a recirculating ice water bath (not shown). The entire apparatus is enclosed in a sealed chamber under a constant flow of N_2 to prevent condensation.

3. Dynamic of crack propagation

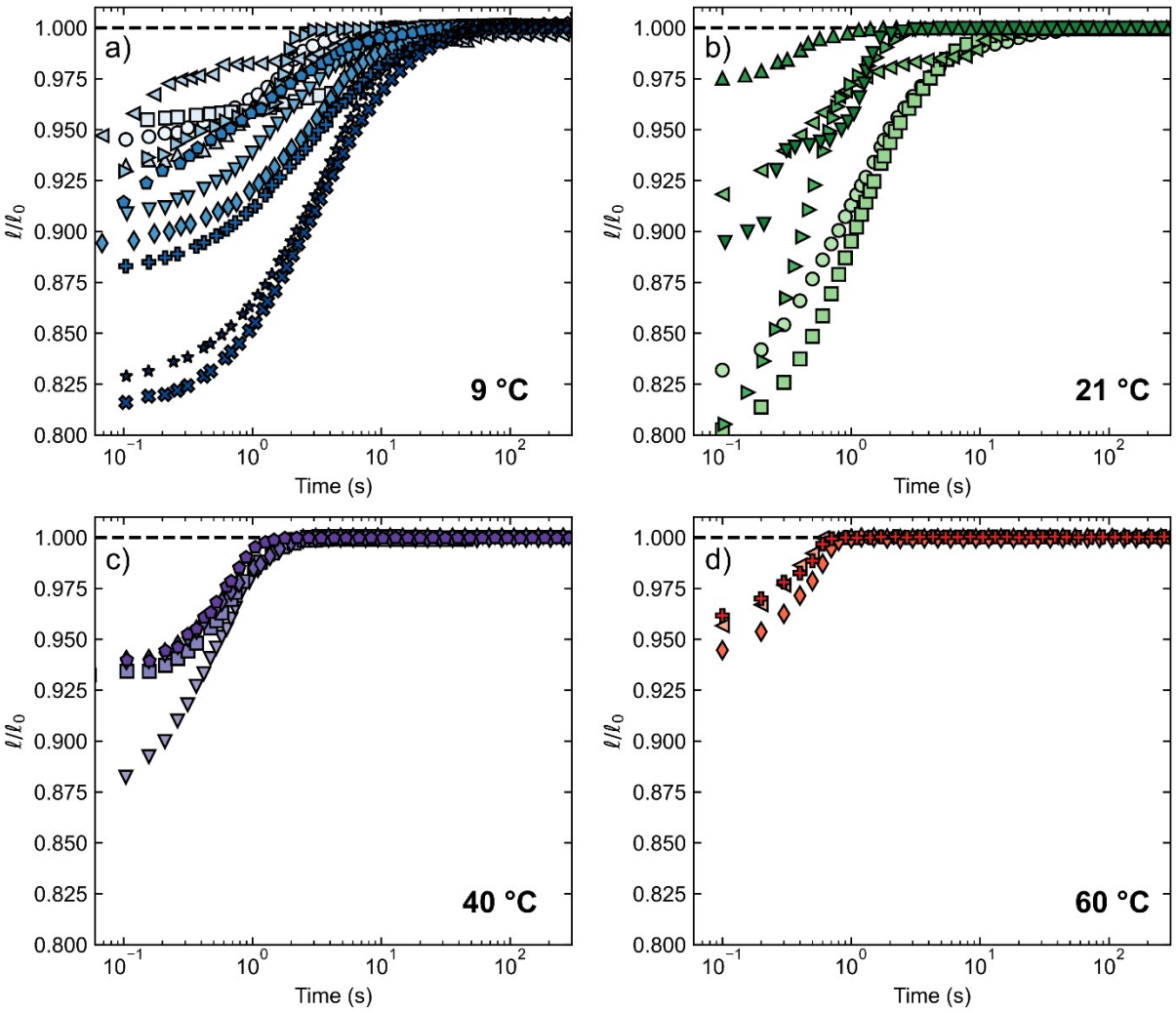

Figure S3. Crack propagation dynamics of DGEBA-Tris. Crack length (normalized by equilibrium crack length) vs time curves for fully cured DGEBA-Tris as a function of temperature, including 9 °C (a), 21 °C (b), 40 °C (c), and 60 °C (d). Dashed line indicates $l = l_0$. Symbols are included to differentiate between experiments, but do not correlate between subfigures.

4. Differential Scanning Calorimetry

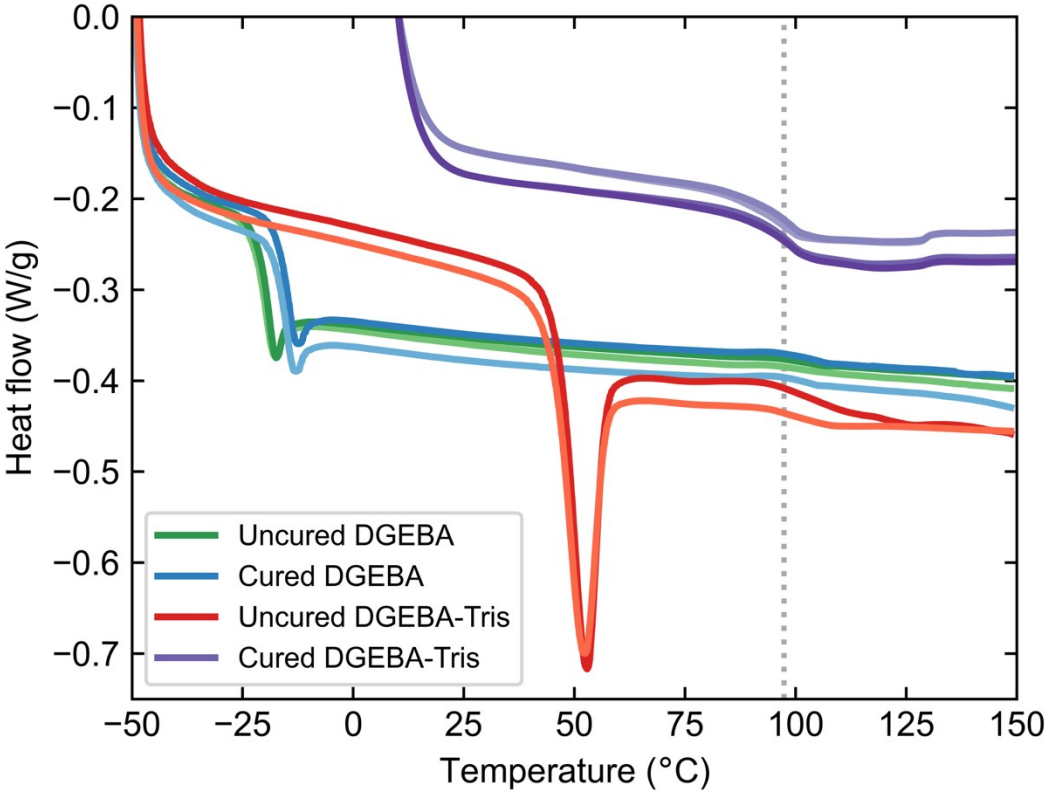

Figure S4. Glass transition temperature of DGEBA and DGEBA-Tris. Differential scanning calorimetry curves of uncured DGEBA (green), DGEBA cured at 220 °C for 48 hours (blue), uncured DGEBA-Tris (red), and DGEBA-Tris cured at 200 °C for 4 hours (purple). Only a minor shift in T_g is observed for thermal curing of DGEBA. The cured DGEBA-Tris curves display a distinct transition centered at 97.3 °C (dotted line), indicative of a glass transition that is significantly higher than the uncured DGEBA-Tris samples.

5. Fitting of $\sqrt{G_c - G_0}$ vs $ln(v)$.

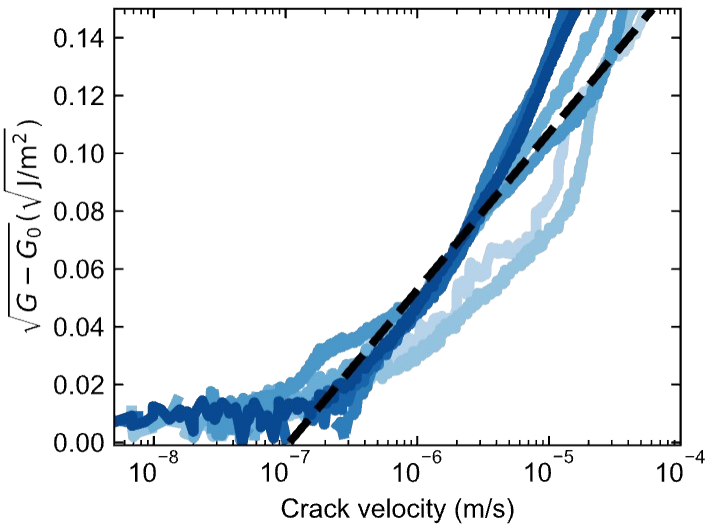

Figure S5. Linear regression of rate-dependent peeling of DGEBA-Tris at 9 °C. Regression of scaled adhesion vs peeling velocity data to **Eqn. 2**. Data from 10^{-7} – 10^{-5} m/s were considered. Regression gives $r^2 = 0.80$, $\frac{M}{n} = 0.256 \pm 0.007$ μN/m, and $\Sigma = 6.0 \pm 0.2 \times 10^{11}$ #/m^2 with $n = 1$.